

# The Electronic Spectra of CH<sub>2</sub>XOH (X = F, Cl, Br): A Comparative Study

Melanie Schnell,<sup>†,‡</sup> Max Mühlhäuser,<sup>†,§</sup> Antonija Lesar,<sup>⊥</sup> and Sigrid D. Peyerimhoff<sup>\*,†</sup>

*Institut für Physikalische und Theoretische Chemie der Universität Bonn, Wegelerstrasse 12, 53115 Bonn, Germany, Institut für Physikalische Chemie und Elektrochemie der Universität Hannover, Callinstrasse 3-3a, 30167 Hannover, Germany, Fachbereich Biologie, Chemie und Werkstoffkunde der Fachhochschule Bonn-Rhein-Sieg, von-Liebig-Strasse 20, 53359 Rheinbach, Germany, and Department of Physical and Organic Chemistry, “Jozef Stefan” Institute, Jamova 39, SI-1000 Ljubljana, Slovenia*

Received: April 21, 2003

Excited states of the halogenated methanol derivatives CH<sub>2</sub>XOH (X = F, Cl, Br) relevant to atmospheric chemistry are investigated with use of ab initio multireference configuration interaction (MRD-CI) calculations. For CH<sub>2</sub>FOH three characteristic dipole allowed transitions were computed:  $1^1A'' \leftarrow X^1A'$  at 7.89 eV,  $2^1A'' \leftarrow X^1A'$  at 9.03 eV, and  $3^1A'' \leftarrow X^1A'$  at 10.21 eV. The first dipole allowed transitions in CH<sub>2</sub>ClOH are computed with 1.5 eV lower excitation energies (at 7.32 eV ( $1^1A'' \leftarrow X^1A'$ ) and around 8 eV ( $2^1A' \leftarrow X^1A'$  and  $2^1A'' \leftarrow X^1A'$ )). The first transitions in CH<sub>2</sub>BrOH are calculated with excitation energies of 6.29 ( $1^1A'' \leftarrow X^1A'$ ), 6.67 ( $2^1A' \leftarrow X^1A'$ ), and 7.59 eV ( $2^1A'' \leftarrow X^1A'$ ). These differences can be understood due to the influence of the different charge distributions at the halogen atoms.

## Introduction

The massive seasonal depletion of ozone<sup>1</sup> in the Arctic troposphere and in the Antarctic during the spring centered great interest on the role of chlorinated species in those regions. Analogous to the importance of chlorine species for the chemistry of the ozone layer are the interactions of stratospheric bromine species.<sup>2,3</sup> It is well-known that bromine species in the atmosphere are effective not only in the destruction of ozone but also in inhibiting ozone formation by the formation of bromine oxides. In addition, fluorine species are also known to have an important influence on the ozone formation and depletion cycles.<sup>4</sup>

It is well-known that because of their different values of electronegativity comparable fluorine, chlorine, and bromine species show quite different properties. In the present work we want to investigate the three methanol derivatives fluoromethanol (CH<sub>2</sub>FOH), chloromethanol (CH<sub>2</sub>ClOH), and bromomethanol (CH<sub>2</sub>BrOH) to study the different influence of the halogen group on the molecular properties, especially the UV absorption spectra.

Bozzelli et al.<sup>5</sup> published a theoretical study of the geometries and thermochemical properties of several chloromethanol derivatives. We have recently investigated possible photodissociation pathways of chloromethanol (CH<sub>2</sub>ClOH) and bromomethanol (CH<sub>2</sub>BrOH).<sup>6,7</sup> Wang et al.<sup>8</sup> have calculated the geometry and harmonic vibrational frequencies of CH<sub>2</sub>FOH at the UMP2(full)/6-31G\* level and Burk et al.<sup>9</sup> published a theoretical study about the acidity of fluoromethanols and have also calculated the geometry of CH<sub>2</sub>FOH at the MP2/6-31G\* level.

In this study we have performed multireference configuration interaction (MRD-CI) and coupled cluster calculations to investigate the electronic absorption spectra of CH<sub>2</sub>FOH, CH<sub>2</sub>ClOH, and CH<sub>2</sub>BrOH to differentiate between them and to search for general trends in the transition energies of the electronic spectra due to the different electronegativities of the halogens.

## Computational Techniques

To determine the molecular structure all geometrical variables of the species considered were fully optimized by using the DFT-method with the B3LYP functional employing the standard 6-31G\*\* basis set of the GAUSSIAN 98<sup>10</sup> program package. The optimized structures were tested for local minima by checking for possible imaginary values in the vibrational analyses. In a second step the computed structures were re-optimized at the coupled cluster level CCSD(T) including singles, doubles, and a perturbative inclusion of connected triple excitations employing the polarized triple- $\zeta$  cc-pVTZ basis sets from Dunning<sup>11</sup> and the MOLPRO 2000 program package.<sup>12</sup>

The computations of the electronically excited states were performed with the selecting multireference single and double excitation configuration interaction method MRD-CI implemented in the DIESEL program package.<sup>13</sup> The selection of reference configurations can be carried out automatically independent of a chosen summation threshold (here 0.85), which means that the sum of the squared coefficients of all reference configurations selected for each state (root) is above this given threshold of 0.85. From this selected set of reference configurations (mains) all single and double excitations in the form of configuration state functions (CSFs) are generated. From this set all configurations with an energy contribution  $\Delta E(T)$  above a given threshold  $T$  were selected, i.e., the contribution of a configuration larger than this value relative to the energy of the reference set is included in the final wave function. A selection threshold of  $T = 10^{-7}$  hartree was used for all three

\* Address correspondence to this author. FAX +49-0228-739064. E-mail: unt000@uni-bonn.de.

<sup>†</sup> Universität Bonn.

<sup>‡</sup> Universität Hannover.

<sup>§</sup> Fachhochschule Bonn-Rhein-Sieg.

<sup>⊥</sup> “Jozef Stefan” Institute.

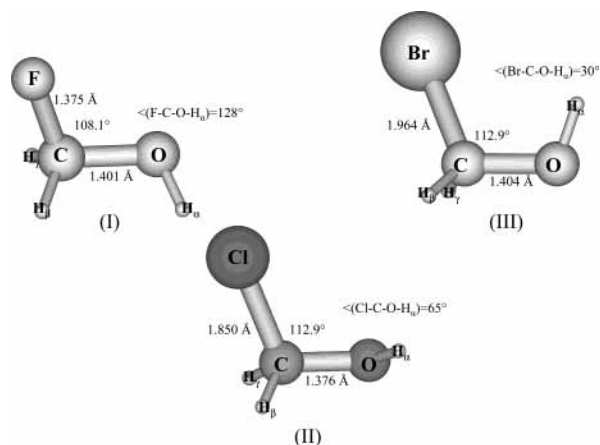


**Figure 1.** Equilibrium geometries of fluoromethanol (**I**), chloromethanol (**II**), and bromomethanol (**III**) in its gauche conformation obtained from our CCSD(T)/cc-pVTZ optimizations as explained in the text.

isomers. The effect of those configurations which contribute less than  $T = 10^{-7}$  hartree is accounted for in the energy computation ( $E(\text{MRD-CI})$ ) by a perturbative technique.<sup>14,15</sup> The contribution of higher excitations is estimated by applying a generalized Langhoff–Davidson correction formula  $E(\text{MRD-CI+Q}) = E(\text{MRD-CI}) + (1 - c_0^2)[E(\text{ref}) - E(\text{MRD-CI})]/c_0^2$ , where  $c_0^2$  is the sum of squared coefficients of the reference species in the total CI wave function and  $E(\text{ref})$  is the energy of the reference configurations.

For the computations of excited states we used a correlation-consistent AO basis set of triple- $\zeta$  quality cc-pVTZ+sp<sup>11</sup> augmented by two d- and one f-polarization functions for carbon, oxygen, and the halogens. In addition this basis set was enlarged by s-Rydberg functions located at the carbon and a negative ion function for the halogen centers. The exponents are  $\alpha_r(\text{C}) = 0.023$  for the s-Rydberg function and  $\alpha_r(\text{F}) = 0.074$ ,  $\alpha_r(\text{Cl}) = 0.049$ , and  $\alpha_r(\text{Br}) = 0.032$  for the negative ion function at the fluorine, chlorine, and bromine centers.

For all three species we have treated 20 electrons active as valence electrons in the CI calculations. The set of reference configurations per IRREP was in the range between 7 and 9 for  $\text{CH}_2\text{FOH}$ , between 8 and 11 for  $\text{CH}_2\text{ClOH}$ , and between 6 and 9 for  $\text{CH}_2\text{BrOH}$ . The number of configuration state functions (CSFs) directly included in the energy calculations is as large as 3.5 million (singlet) and 4.1 million (triplet) for  $\text{CH}_2\text{FOH}$  selected from a total space of 6.3 million (singlet) and 8.9 million (triplet) generated configurations. For  $\text{CH}_2\text{ClOH}$  the number of CSFs is 3.5 million (singlet) and 5.7 million (triplet) out of a total generated space of 6 million (singlet) and 11.4 million (triplet). The number of CSFs for  $\text{CH}_2\text{BrOH}$  is as large as 2.3 million (singlet) and 3.1 million (triplet) from a total space of generated configurations of 6.1 million (singlet) and 7.7 million (triplet).

## Results and Discussion

The calculated equilibrium geometries of the three species  $\text{CH}_2\text{FOH}$ ,  $\text{CH}_2\text{ClOH}$ , and  $\text{CH}_2\text{BrOH}$  can be seen from Figure 1. In Tables 1, 2, and 3 comparisons between our preliminary B3LYP/6-31G\*\* values, the CCSD(T)/cc-p-VTZ optimized values, and structures reported in the literature<sup>5,8,9</sup> for the three investigated species are given. As can be seen, reasonable results for the equilibrium geometries are already obtained at the B3LYP/6-31G\*\* level. In addition our values optimized at different theoretical levels are in good agreement with the calculated values given in the literature.

**TABLE 1: Bond Characteristics of Fluoromethanol  $\text{CH}_2\text{FOH}^a$**

	B3LYP/6-31G**	CCSD(T)/cc-p-VTZ	UMP2/6-31G** <sup>b</sup>
$r(\text{CO})$	1.401	1.381	1.384
$r(\text{CF})$	1.375	1.381	1.390
$r(\text{CH}_\beta) = r(\text{CH}_\gamma)$	1.098	1.093	1.095
$r(\text{OH}_\alpha)$	0.957	0.961	0.972
$\angle\text{COH}_\alpha$	109.2	108.1	108.0
$\angle\text{OCF}$	108.1	111.1	
$\angle\text{OCH}_{\beta/\gamma}$	109.9	112.6	106.6
$\angle\text{FCOH}_\alpha$	128.7	128.4	

<sup>a</sup> The numbering of angles, distances, and atomic centers is according to Figure 1 (structure **I**). The bond lengths are given in Å, angles in degrees. The values have been obtained at various levels of theory (B3LYP, CCSD(T)) as explained in the text. According to the geometry given in Figure 1  $\text{H}_\alpha$  is located gauche to the fluorine and to  $\text{H}_\beta$ . <sup>b</sup> Taken from ref 8 for comparison.

**TABLE 2: Bond Characteristics of Chloromethanol ( $\text{CH}_2\text{ClOH}$ )<sup>a</sup>**

	B3LYP/6-31G**	CCSD(T)/cc-p-VTZ	UMP2/6-31G** <sup>b</sup>
$r(\text{CO})$	1.376	1.381	1.385
$r(\text{CCl})$	1.850	1.808	1.801
$r(\text{CH}_\beta) = r(\text{CH}_\gamma)$	1.094	1.085	1.088
$r(\text{OH}_\alpha)$	0.971	0.959	0.965
$\angle\text{COH}_\alpha$	108.8	108.0	108.2
$\angle\text{OCCl}$	112.9	112.7	
$\angle\text{OCH}_{\beta/\gamma}$	114.2	110.7	107.1
$\angle\text{ClCOH}_\alpha$	67.5	68.3	

<sup>a</sup> The numbering of angles, distances, and atomic centers is according to Figure 1 (structure **II**). The bond lengths are given in Å, angles in degrees. The values have been obtained at various levels of theory (B3LYP, CCSD(T)) as explained in the text. According to the geometry given in Figure 1  $\text{H}_\alpha$  is located gauche to the chlorine and to  $\text{H}_\beta$ . <sup>b</sup> Taken from ref 20 for comparison.

**TABLE 3: Bond Characteristics of Bromomethanol  $\text{CH}_2\text{BrOH}$ <sup>a</sup>**

	B3LYP/6-31G**	CCSD(T)/cc-p-VTZ
$r(\text{CO})$	1.404	1.382
$r(\text{CBr})$	1.964	1.984
$r(\text{CH}_\beta) = r(\text{CH}_\gamma)$	1.092	1.088
$r(\text{OH}_\alpha)$	0.965	0.962
$\angle\text{COH}_\alpha$	109.4	108.2
$\angle\text{OCBr}$	112.9	112.9
$\angle\text{OCH}_{\beta/\gamma}$	111.9	114.1
$\angle\text{BrCOH}_\alpha$	29.7	30.3

<sup>a</sup> The numbering of angles, distances, and atomic centers is according to Figure 1 (structure **III**). The bond lengths are given in Å, angles in degrees. The values have been obtained at various levels of theory (B3LYP, CCSD(T)). According to the geometry given in Figure 1  $\text{H}_\alpha$  is located gauche to the bromine and to  $\text{H}_\beta$ .

The global minimum of  $\text{CH}_2\text{XOH}$  ( $X = \text{F}, \text{Cl}, \text{Br}$ ) is characterized by  $C_1$ -symmetry with  $\text{H}_\alpha$  gauche to the C–O–X frame ( $X = \text{halogen atom}$ ) with an out-of-plane angle ( $\angle\text{X–C–O–H}_\alpha$ ) of about  $128^\circ$  for  $\text{CH}_2\text{FOH}$  (Table 1), about  $65^\circ$  for  $\text{CH}_2\text{ClOH}$  (Table 2), and about  $30^\circ$  for  $\text{CH}_2\text{BrOH}$  (Table 3). Rotation of the OH group leads to the competing cis ( $\angle\text{X–C–O–H}_\alpha = 0^\circ$ ) and trans conformers ( $\angle\text{X–C–O–H}_\alpha = 180^\circ$ ). But the asymmetric structure is expected to be energetically favored relative to these cis and trans conformers due to the anomeric effect that has been found for chloromethanol ( $\text{CH}_2\text{ClOH}$ ) in former studies.<sup>6,16</sup>

In Table 4 the energy differences between the cis, trans, and gauche conformers of the three species  $\text{CH}_2\text{XOH}$  ( $X = \text{F}, \text{Cl}, \text{Br}$ ) are given at different theoretical levels. As can be seen the results of the several calculations are in good agreement with

**TABLE 4:** Calculated Energy Differences (in kcal/mol) between *Gauche*, *Cis*, and *Trans* Conformers of CH<sub>2</sub>FOH, CH<sub>2</sub>ClOH, and CH<sub>2</sub>BrOH at Various Levels As Explained in the Computational Techniques<sup>a</sup>

	CH <sub>2</sub> FOH		CH <sub>2</sub> ClOH		CH <sub>2</sub> BrOH	
	cis	trans	cis	trans	cis	trans
B3LYP/6-31G**	2.9	5.2	2.5	4.9	3.6	6.5
CCSD(T)/cc-p-VTZ	3.2	4.7	2.3	4.7	2.7	4.6
E(MRD-CI)/cc-p-VTZ+sp	2.7	4.3	2.1	4.9	2.4	4.3
E(MRD-CI+Q)/cc-p-VTZ+sp	2.2	3.9	1.9	4.8	1.8	4.1

<sup>a</sup> The values are relative to the global minimum (*gauche* structures).

**TABLE 5:** Calculated Transition Energies  $\Delta E$  [eV] from the Ground States X<sup>1</sup>A' of the C<sub>s</sub>-Symmetric *Cis* Conformers of CH<sub>2</sub>XOH (X = F, Cl, Br) to the Lowest Singlet States and Comparison with the Corresponding Transitions in *gauche*-CH<sub>2</sub>XOH (X = F, Cl, Br)<sup>a</sup>

<i>cis</i> -CH <sub>2</sub> FOH			<i>gauche</i> -CH <sub>2</sub> FOH	
state	excitation	$\Delta E$ [eV]	state	$\Delta E$ [eV]
X <sup>1</sup> A'	(7a') <sup>2</sup> (3a'') <sup>2</sup>	0.0	X <sup>1</sup> A	0.0
1 <sup>1</sup> A''	3a'' → 8a'	7.89	2 <sup>1</sup> A	8.08
2 <sup>1</sup> A''	3a'' → 9a'	9.03	3 <sup>1</sup> A	9.13
3 <sup>1</sup> A''	3a'' → 10a'	10.21	4 <sup>1</sup> A	10.13

<i>cis</i> -CH <sub>2</sub> ClOH			<i>gauche</i> -CH <sub>2</sub> ClOH	
state	excitation	$\Delta E$ [eV]	state	$\Delta E$ [eV]
X <sup>1</sup> A'	(7a') <sup>2</sup> (3a'') <sup>2</sup>	0.0	X <sup>1</sup> A	0.0
1 <sup>1</sup> A''	3a'' → 8a'	7.32	2 <sup>1</sup> A	7.26
2 <sup>1</sup> A''	7a' → 8a'	7.95	3 <sup>1</sup> A	7.75
2 <sup>1</sup> A''	3a'' → 9a'	7.98	4 <sup>1</sup> A	8.00

<i>cis</i> -CH <sub>2</sub> BrOH			<i>gauche</i> -CH <sub>2</sub> BrOH	
state	excitation	$\Delta E$ [eV]	state	$\Delta E$ [eV]
X <sup>1</sup> A'	(7a') <sup>2</sup> (3a'') <sup>2</sup>	0.0	X <sup>1</sup> A	0.0
1 <sup>1</sup> A''	3a'' → 8a'	6.29	2 <sup>1</sup> A	6.34
2 <sup>1</sup> A''	7a' → 8a'	6.67	3 <sup>1</sup> A	6.52
2 <sup>1</sup> A''	3a'' → 9a'	7.59	4 <sup>1</sup> A	7.55
3 <sup>1</sup> A''	3a'' → 10a'	7.62	5 <sup>1</sup> A	7.71

<sup>a</sup> The excitation energies are given with respect to the lowest state of each conformer. The values have been obtained at the MRD-CI+Q/cc-pVTZ+sp level as explained in the computational techniques.

each other. On the MRD-CI+Q level the asymmetric global minimum structure is about 2 kcal/mol below the *cis* structure in C<sub>s</sub>-symmetry and the *trans* conformer is higher in energy by about 4 kcal/mol for all three species.

To investigate whether the OH rotation has a large influence on the electronic absorption spectrum we calculated transition energies to the lowest excited singlet states of the *gauche* and the low-lying *cis* conformers for CH<sub>2</sub>XOH (X = F, Cl, Br). In Table 5 we summarize the results. With respect to the 20 electrons treated active in the CI calculations as valence electrons the ground-state configuration of CH<sub>2</sub>XOH (X = F, Cl, Br) is (7a')<sup>2</sup>(3a'')<sup>2</sup> (*cis*) and (10a')<sup>2</sup> (*gauche*). The calculated spectra of the *gauche* and *cis* conformers are very similar for all three species. The excitation energies obtained show only minor changes. Because computations in C<sub>s</sub>-symmetry are more economic than without symmetry restriction and qualitative conclusions concerning MO considerations are more easily drawn if symmetry is involved we will restrict the following discussion of the electronic spectra of CH<sub>2</sub>XOH (X = F, Cl, Br) to the C<sub>s</sub>-symmetric *cis* conformers which lie less than 2 kcal/mol above the absolute minima (Table 4). However, the general conclusions will also be valid for the asymmetric *gauche* conformation as can be seen from Table 5 in which the lowest excitations of *cis* and *gauche* structures are compared.

**TABLE 6:** Calculated Electronic Transition Energies  $\Delta E$  [eV] and Oscillator Strengths  $f$  from the Ground State X<sup>1</sup>A' of C<sub>s</sub>-Symmetric *cis*-CH<sub>2</sub>FOH to Its Low-Lying Electronic States<sup>a</sup>

state	excitation	$\Delta E$ [eV]	$f$
X <sup>1</sup> A'	(7a') <sup>2</sup> (3a'') <sup>2</sup>	0.0	
1 <sup>3</sup> A''	3a'' → 8a'	7.77	
1 <sup>1</sup> A''	3a'' → 8a'	7.89	0.001
2 <sup>3</sup> A''	3a'' → 9a'	8.72	
2 <sup>1</sup> A''	3a'' → 9a'	9.03	0.05
3 <sup>3</sup> A''	3a'' → 10a'	10.0	
3 <sup>1</sup> A''	3a'' → 10a'	10.21	0.005
1 <sup>3</sup> A'	3a'' → 4a''	10.28	
2 <sup>3</sup> A'	7a' → 8a'	10.29	

<sup>a</sup> The excitation energies are given with respect to the lowest state of each species. The ground state configuration for the valence electrons is (7a')<sup>2</sup>(3a'')<sup>2</sup> due to the 20 electrons treated active in the CI calculations as explained in the text. The values have been obtained at the MRD-CI+Q/cc-p-VTZ+sp level as explained in the computational techniques.

**TABLE 7:** Calculated Electronic Transition Energies  $\Delta E$  [eV] and Oscillator Strengths  $f$  from the Ground State X<sup>1</sup>A' of C<sub>s</sub>-Symmetric *cis*-CH<sub>2</sub>ClOH to Its Low-Lying Electronic States and Comparison with the Corresponding Transitions in *cis*-CH<sub>2</sub>BrOH<sup>a</sup>

state	excitation	<i>cis</i> -CH <sub>2</sub> ClOH		<i>cis</i> -CH <sub>2</sub> BrOH	
		$\Delta E$ [eV]	$f$	$\Delta E$ [eV]	$f$
X <sup>1</sup> A'	(7a') <sup>2</sup> (3a'') <sup>2</sup>	0.0		0.0	
1 <sup>3</sup> A''	3a'' → 8a'	6.86		5.84	
1 <sup>3</sup> A'	7a' → 8a'	7.09		6.11	
1 <sup>1</sup> A''	3a'' → 8a'	7.32	0.0003	6.29	0.0004
2 <sup>3</sup> A''	3a'' → 9a'	7.67		7.44	
2 <sup>1</sup> A'	7a' → 8a'	7.95	0.002	6.67	0.01
2 <sup>1</sup> A''	3a'' → 9a'	7.98	0.01	7.59	0.02
3 <sup>3</sup> A''	2a'' → 8a'	8.21		7.54	
2 <sup>3</sup> A'	6a' → 8a'	8.44		7.37	
3 <sup>1</sup> A''	2a'' → 8a'	8.45	0.001	7.62	0.03

<sup>a</sup> The excitation energies are given with respect to the lowest state of each species. The ground state configuration for the valence electrons is (7a')<sup>2</sup>(3a'')<sup>2</sup> due to the 20 electrons treated active in the CI calculations as explained in the text. The values have been obtained at the MRD-CI+Q/cc-pVTZ+sp level as explained in the computational techniques.

In Tables 6 and 7 we present a comparison of the computed excitation energies and transition probabilities between *cis*-CH<sub>2</sub>-FOH, *cis*-CH<sub>2</sub>ClOH, and *cis*-CH<sub>2</sub>BrOH. The ground states of these CH<sub>2</sub>XOH species (X = F, Cl, Br) are singlet states. Because of spin conservation transitions to singlet excited states are most likely but recent experimental photodissociation studies have shown that spin-orbit coupling has a nonnegligible influence for some halogen species such as HOCl so that weak transitions to triplet states are possible.<sup>17,18</sup> Because of this we have also considered triplet states as shown in Tables 6 and 7.

For fluoromethanol (CH<sub>2</sub>FOH, Table 6) besides the HOMO-LUMO excitation 3a'' → 8a' also transitions from the HOMO into other virtual orbitals (9a', 10a') are found to play an important role in the electronic spectrum. The HOMO-LUMO excitation leads to the two states 1<sup>1</sup>A'' and 1<sup>3</sup>A'' which are calculated at 7.89 (1<sup>1</sup>A'') and 7.77 eV (1<sup>3</sup>A''). The computed oscillator strength  $f$  for the singlet transition is 0.001. In Figure 2 characteristic molecular orbitals (MOs) of fluoromethanol are presented. The HOMO 3a'' shows mainly dominant  $\pi^*(C-O)$ -antibonding character and relatively little  $\pi^*(C-F)$  (C-F antibonding) contributions from the fluorine. The LUMO 8a' has mainly diffuse character with little nonbonding contribution ( $n(F-C-O)$ ). Therefore this transition can be primarily characterized as an excitation into a diffuse upper orbital. The

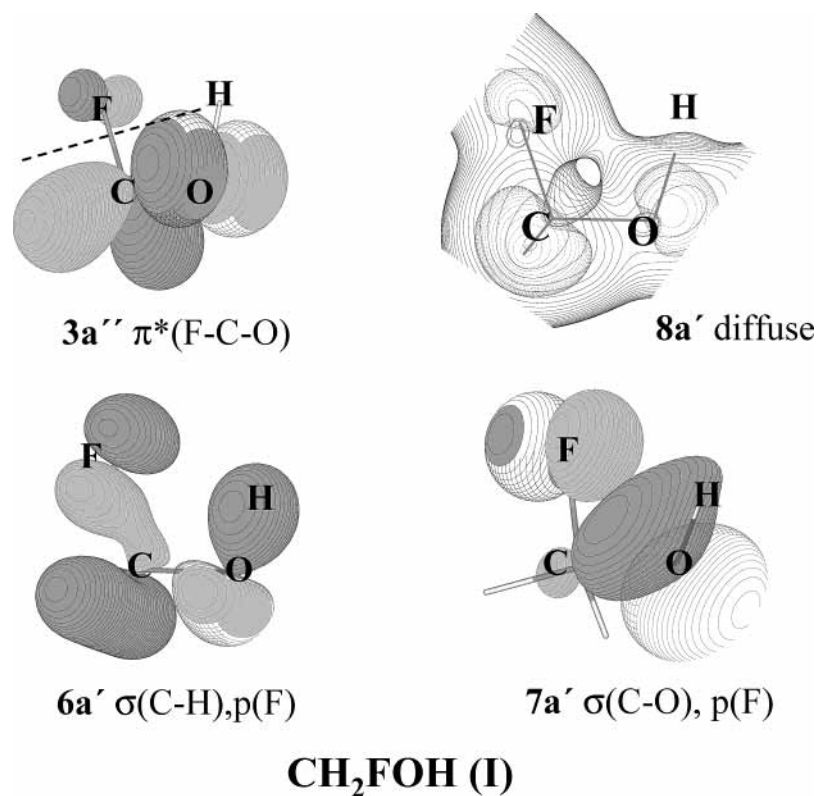


**Figure 2.** Charge density contours of characteristic occupied valence orbitals ( $6a'$ ,  $7a'$ ,  $3a''$ ) and the lowest virtual molecular orbital LUMO ( $8a'$ ) of  $\text{CH}_2\text{FOH}$ .

singlet–triplet splitting for the two states is calculated to be only 0.12 eV. This is also a strong indication that the LUMO  $8a'$  has substantial Rydberg character or has very little overlap with the lower orbital  $3a''$ .

The next excitation with nonzero oscillator strength is computed at 9.03 eV ( $2^1A''$ ) with an  $f$ -value of 0.05 corresponding to a  $3a'' \rightarrow 9a'$  excitation and a singlet–triplet splitting of 0.31 eV. The  $9a'$  shows a lone-pair p function at the fluorine with additional diffuse contributions. The  $3a'' \rightarrow 10a'$  excitation leads to states computed at 10.21 eV ( $1^1A''$ ) and 10.0 eV ( $3^1A''$ ). The oscillator strength for the singlet transition is computed with 0.005.

In chloromethanol ( $\text{CH}_2\text{ClOH}$ ) and bromomethanol ( $\text{CH}_2\text{BrOH}$ , Table 7) the  $3a'' \rightarrow 8a'$  HOMO–LUMO and  $3a'' \rightarrow 9a'$  transitions are shifted distinctly to lower energies so that the lowest energy singlet transition is calculated at 7.32 eV in chloromethanol and at 6.29 eV in  $\text{CH}_2\text{BrOH}$ , 0.57 and 1.6 eV lower, respectively, than in the fluorinated compound. The  $8a'$  MO seems to have somewhat less diffuse character in  $\text{CH}_2\text{ClOH}$  and  $\text{CH}_2\text{BrOH}$  compared to  $\text{CH}_2\text{FOH}$  measured by the larger singlet–triplet splitting between the  $A''$  ( $3a'' \rightarrow 8a'$ ) states in the heavier systems. The decrease in the energy of the more intense  $3a'' \rightarrow 9a'$  transitions is of similar magnitude in going from the fluoro- to the chloro- and finally to bromomethanol. But more important is the finding that transitions from the outer valence orbitals  $7a'$ ,  $6a'$ , and  $2a''$  into the LUMO  $8a'$  are also seen to lie in the lower energy region for  $\text{CH}_2\text{ClOH}$  and  $\text{CH}_2\text{BrOH}$ . A more detailed discussion of the most important features of the electronic absorption spectrum of  $\text{CH}_2\text{ClOH}$  has been reported earlier.<sup>6</sup>

The excitation  $7a' \rightarrow 8a'$  is calculated at 7.09 ( $3^1A'$ ) and 7.95 eV ( $1^1A'$ ) in  $\text{CH}_2\text{ClOH}$  and at 6.11 and 6.67 eV, respectively, in  $\text{CH}_2\text{BrOH}$ . The  $7a'$  orbital can be characterized to a large extent as a lone pair on chlorine in  $\text{CH}_2\text{ClOH}$ , and the  $8a'$  as  $\sigma^*(\text{C}-\text{Cl})$  antibonding orbital. As seen in Figure 3 the charge densities

of the upper MOs are very similar in  $\text{CH}_2\text{ClOH}$  and  $\text{CH}_2\text{BrOH}$ . Hence the  $7a' \rightarrow 8a'$  excitation in both compounds can be considered as an  $n \rightarrow \sigma^*$  type transition. Since both orbitals,  $7a'$  and  $8a'$ , have their charge density maxima in the same plane, the singlet–triplet splitting for the corresponding states is relatively large (0.86 eV for the chloro and 0.56 eV for the bromo compound). In  $\text{CH}_2\text{BrOH}$  the  $3a''$  MO can also be described mainly as a (out of plane) bromine lone pair, and hence the location of  $3a'' \rightarrow 8a'$  ( $3^1A''$ ) and  $7a' \rightarrow 8a'$  ( $3^1A'$ ) states in a similar energy range (with a smaller singlet–triplet splitting for the states resulting from the out-of-plane transition) is conceivable. The situation is entirely different in fluoromethanol (Figure 2). The  $7a'$  has a large C–O bonding contribution in addition to the charge on fluorine and is therefore much lower in energy relative to its  $3a''$  MO. As a consequence the  $3^1A'$  ( $7a' \rightarrow 8a'$ ) in  $\text{CH}_2\text{FOH}$  is calculated at 10.29 eV and the large singlet–triplet splitting would place the corresponding singlet presumably above 11 eV.

The major differences in the electronic absorption spectra of  $\text{CH}_2\text{FOH}$ ,  $\text{CH}_2\text{ClOH}$ , and  $\text{CH}_2\text{BrOH}$  can be understood on the basis of simple MO theory leading to the different values of electronegativity of the halogen compounds. Fluorine has an electronegativity of 4.10 (after Allred–Rochow<sup>19</sup>), the value for chlorine is 2.83, and that for bromine is 2.74. Simple MO theory predicts a larger effective charge for 2p electrons in fluorine than for 3p and 4p electrons in chlorine and bromine, respectively. In other words 2p electrons in fluorine are more tightly bound (lower orbital energy) than the valence p electrons in the chlorine atom and even more so than the electrons in the bromine 4p shell. Therefore MOs with a large influence of a fluorine substituent should be lower in energy than the corresponding MOs with a chlorine substituent. In addition, for a MO that has large halogen character the energy lowering should be more significant than that for another MO of the same molecule with only a small or no halogen character. Bromine

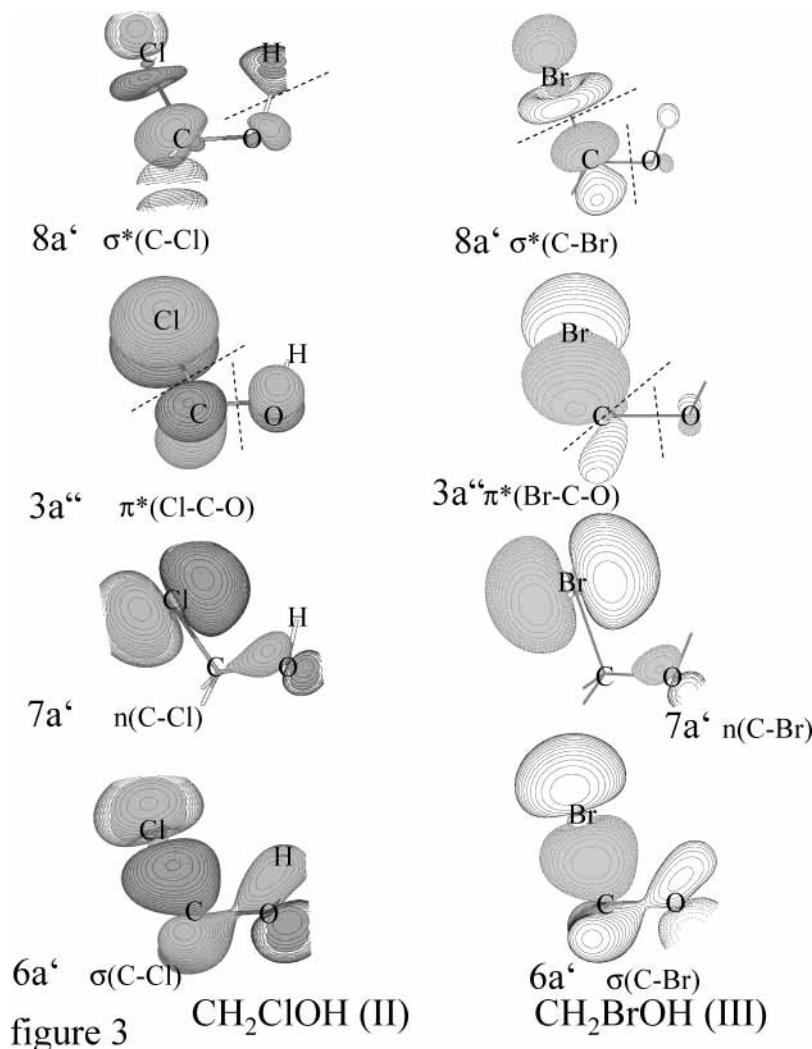


**Figure 3.** Charge density contours of characteristic occupied valence orbitals ( $6a'$ ,  $7a'$ ,  $3a''$ ) and the lowest virtual molecular orbital LUMO ( $8a'$ ) of CH<sub>2</sub>ClOH (**II**) and CH<sub>2</sub>BrOH (**III**).

has the smallest electronegativity of the three halogens considered in this study. Consequently the effects for CH<sub>2</sub>BrOH are expected to be somewhat smaller than those for CH<sub>2</sub>ClOH or CH<sub>2</sub>FOH.

The charge densities in Figures 2 and 3 show that all high-lying orbitals have considerable contributions from the halogens. The HOMOs  $3a''$  show the largest resemblance with one another. Its orbital binding energy decreases from the fluorine to the bromine compound. As a result the HOMO-LUMO gap becomes smaller from CH<sub>2</sub>FOH to CH<sub>2</sub>ClOH and CH<sub>2</sub>BrOH and the first triplet states ( $^3A''$ ) are found at 7.77, 6.84, and 5.84 eV, respectively, while the dipole-allowed transitions are at 7.89, 7.32, and 6.29 eV for the weak and at 9.03, 7.98, and 7.59 eV for the more intense absorption. The  $7a'$  is much lower in CH<sub>2</sub>FOH than in the other two molecules because of mixing with F(2p) and CO bonding. For this reason the CH<sub>2</sub>FOH spectrum is dominated by excitations from the  $3a''$  in unoccupied orbitals while transitions from orbitals below the HOMO are also in the lower energy region only in CH<sub>2</sub>ClOH and CH<sub>2</sub>BrOH.

From our study it is clear that the best possibility to differentiate between CH<sub>2</sub>FOH, CH<sub>2</sub>ClOH, and CH<sub>2</sub>BrOH is the lower energy window below 7 eV because there are only dipole allowed transitions of CH<sub>2</sub>BrOH. The electronic spectrum of CH<sub>2</sub>ClOH shows characteristic fingerprints around 8 eV while

for CH<sub>2</sub>FOH we have computed a strong transition in the far-UV around 9 eV.

### Summary and Conclusions

Multireference configuration interaction (MRD-CI) calculations are employed to investigate the electronic spectra of CH<sub>2</sub>XOH (X = F, Cl, Br) to determine the influence of the different electronegativities of the halogen substituents and to differentiate between these species. The ground-state equilibrium geometries of CH<sub>2</sub>XOH are found to be gauche but we calculated the *C<sub>s</sub>*-symmetric cis conformers of all three species only about 2 kcal/mol higher in energy.

For CH<sub>2</sub>FOH we find three characteristic dipole-allowed transitions below 10.5 eV:  $1^1A'' \leftarrow X^1A'$  at 7.89 eV,  $2^1A'' \leftarrow X^1A'$  at 9.03 eV, and  $3^1A'' \leftarrow X^1A'$  at 10.21 eV. In contrast the corresponding low-lying transitions of CH<sub>2</sub>ClOH are computed at 7.32 ( $1^1A'' \leftarrow X^1A'$ ), 7.95 ( $2^1A' \leftarrow X^1A'$ ), and 7.98 eV ( $2^1A'' \leftarrow X^1A'$ ), i.e., at about 0.5 to 1.0 eV lower transition energies. Furthermore for CH<sub>2</sub>BrOH we calculated the first dipole allowed transitions at 6.29 ( $1^1A'' \leftarrow X^1A'$ ), 6.67 ( $2^1A' \leftarrow X^1A'$ ), and 7.59 eV ( $2^1A'' \leftarrow X^1A'$ ), again about 1 to 1.4 eV lower. These differences can be understood from qualitative MO considerations. The different electronegativity or stability of atomic orbitals of the halogen substituents fluorine, chlorine, and bromine strongly influences the occupied valence orbitals as

the HOMO  $3a''$  and  $7a'$ . MOs ( $X = F, Cl, Br$ ) consisting of a strong halogen character will be lower in energy the more electronegative the halogen partner is. Thus the HOMO-LUMO gap in  $CH_2FOH$  is larger than that in  $CH_2XOH$  ( $X = Cl, Br$ ), resulting in higher excitation energies for the first transitions in  $CH_2FOH$ .

**Acknowledgment.** The present study is part of the NATO science project Study of elementary steps of radical reactions in atmospheric chemistry. The financial support from the NATO collaborative linkage grant Environmental Earth Science and Technology (EST.CLG.977083) is gratefully acknowledged. M. Hanrath is thanked for various improvements of the DIESEL program package. M.S. acknowledges a grant from the Fonds der chemischen Industrie.

## References and Notes

- (1) Farman, J. C.; Gardiner, B. G.; Shanklin, J. D. *Nature* **1985**, *315*, 207.
- (2) Wolfsy, S. C.; McElroy, M. B.; Yung, Y. L. *Geophys. Res. Lett.* **1975**, *2*, 215.
- (3) Vogt, R.; Crutzen, P. J.; Sander, R. *Nature* **1996**, *383*, 327.
- (4) Hollemann, A. F.; Wiberg, E. *Lehrbuch der Anorganischen Chemie*, 101 Auflage; de Gruyter: Berlin, New York, 1995; pp 519.
- (5) Sun, H.; Bozzelli, J. W. *J. Phys. Chem. A*, **2001**, *105*, 4504.
- (6) Mühlhäuser, M.; Schnell, M.; Peyerimhoff, S. D. *Mol. Phys.* **2002**, *100*, 509. Schnell, M.; Mühlhäuser, M.; Peyerimhoff, S. D. *Chem. Phys. Lett.* **2001**, *344*, 519.
- (7) Lesar, A.; Schnell, M.; Mühlhäuser, M.; Peyerimhoff, S. D. *Chem. Phys. Lett.* **2002**, *366*, 350.
- (8) Wang, B.; Hou, H.; Gu, Y. *Chem. Phys. Lett.* **1999**, *300*, 99.
- (9) Burk, P.; Koppel, I. A.; Rummel, A.; Trummel, A. *J. Phys. Chem. A* **2000**, *104*, 1602.
- (10) Frisch, M. J.; Trucks, G. W.; Schlegel, H. B.; Gill, P. M. W.; Johnson, B. G.; Robb, M. A.; Cheeseman, J. R.; Keith, T. A.; Peterson, G. A.; Montgomery, J. A.; Raghavachari, K.; Al-Laham, M. A.; Zakrewski, V. G.; Ortiz, J. V.; Foresman, J. B.; Cioslowski, J.; Stefanov, B. B.; Nanayakkara, A.; Challacombe, M.; Peng, C. Y.; Ayala, P. Y.; Chen, W.; Wong, M. W.; Andres, J. L.; Replogle, E. S.; Matrin, R. L.; Fox, D. J.; Binkley, J. S.; Defrees, D. J.; Baker, J.; Stewart, J. P.; Head-Gordon, M.; Gonzales, C.; Pople, J. A. *Gaussian 98*; Gaussian Inc.: Pittsburgh, PA, 1999.
- (11) Dunning, T. H., Jr. *J. Chem. Phys.* **1989**, *90*, 1007. Woon, D. E.; Dunning, T. H., Jr. *J. Chem. Phys.* **1993**, *98*, 1358.
- (12) *MOLPRO 2000*. a package of ab initio programs written by Werner, H.-J.; Knowles, P. J. with contributions from Amos, R. D.; Bernhardsson, A.; Berning, A.; Celanie, P.; Cooper, D. L.; Deegan, M. J. O.; Dobbyn, A. J.; Eckert, F.; Hampel, C.; Hetzer, G.; Korona, T.; Lindh, R.; Lloyd, A. W.; Mc Nicholas, S. J.; Manby, F. R.; Meyer, W.; Mura, M. E.; Nicklass, A.; Palmieri, P.; Pitzer, R.; Rauhut, G.; Schutz, M.; Stoll, H.; Stone, A. J.; Tarroni, R.; Thorsteinsson, T.
- (13) Hanrath, M.; Engels, B. *Chem. Phys.* **1997**, *225*, 197.
- (14) Buenker, R. J.; Peyerimhoff, S. D. *Theor. Chim. Acta* **1974**, *35*, 33.
- (15) Buenker, R. J.; Peyerimhoff, S. D. *Theor. Chim. Acta* **1975**, *39*, 217.
- (16) Omoto, K.; Marusani, K.; Hirao, H.; Imade, M.; Fujimoto, H. *J. Phys. Chem. A* **2000**, *104*, 6499.
- (17) Barnes, R. J.; Lock, M.; Coleman, J.; Sinha, A. *J. Phys. Chem. A* **1996**, *100*, 453.
- (18) Francisco, J. S.; Hand, M. R.; Williams, I. H. *J. Phys. Chem. A* **1996**, *100*, 9250.
- (19) Hollemann, A. F.; Wiberg, E. *Lehrbuch der Anorganischen Chemie*, 101 Auflage; de Gruyter: Berlin, New York, 1995; p 144, Table 20.